Theoretical study on the spin-state transition in doped $La_{2-x}Sr_xCoO_4$

2000 J. Phys.: Condens. Matter 12 7425

(http://iopscience.iop.org/0953-8984/12/33/310)

J. Phys.: Condens. Matter **12** (2000) 7425–7432. Printed in the UK PII: S0953-8984(00)14844-1

Theoretical study on the spin-state transition in doped $La_{2-x}Sr_xCoO_4$

J Wang, Y C Tao, Weiyi Zhang and D Y Xing

National Laboratory of Solid State Microstructures and Department of Physics, Nanjing University, Nanjing 210093, China

Received 20 June 2000

Abstract. The spin-state transition is an interesting and unresolved problem in layered perovskite $La_{2-x}Sr_xCoO_4$ under doping, as it involves competition among different magnetic structures. Within the unrestricted Hartree–Fock approximation and using the real space recursion method we have studied the effect of Sr doping on the magnetic and electronic properties of layered perovskite La_2CoO_4. All configurations in an enlarged double cell among the low-spin ($t_{2g}^6e_g^1$) and the high-spin ($t_{2g}^5e_g^2$) states are considered. It is found that the ground state of a doped system takes the antiferromagnetic high-spin state ($t_{2g}^{5-x}e_g^2$) for $0 < x < 0.39$, the ferromagnetic high-spin state ($t_{2g}^5e_g^{2-x}$) for $0.39 \leqslant x < 0.52$, followed by the ferromagnetic high-spin–low-spin ordered state ($t_{2g}^{5-x}e_g^2$–$t_{2g}^6e_g^{1-x}$) for $0.52 \leqslant x < 1.1$. The two spin-state transitions in the doping range ($0 < x < 1.1$) we studied are in agreement with experimental observations.

1. Introduction

Recently, there has been much debate [1] concerning the anomalous spin-state transition of $La_{1-x}Sr_xCoO_3$ as well as its complex electronic and magnetic properties. Both photoemission spectra [2] and electrical resistivity measurements [3] on this doped system have revealed that there appears to be an insulator–metal transition at a doping concentration of $x \sim 0.2$; moreover, this transition is often accompanied by a magnetic transition from the nonmagnetic state to the ferromagnetically ordered state. To explore the nature of such a spin-state transition in the doped compound, Zhuang *et al* [4] have calculated the electronic structure of $La_{1-x}Sr_xCoO_3$ for the whole doping range $0.0 < x < 1.0$ and found that the ground state changes from the low-spin state ($t_{2g}^{6-x}e_g^0$) at low doping concentration $x < 0.25$ to a ferromagnetic intermediate-spin state ($t_{2g}^5e_g^{1-x}$) for moderate doping $0.25 \leqslant x < 0.41$; for a higher doping concentration $0.41 \leqslant x < 0.95$ the ground state of the system takes an intermediate-spin–high-spin ($t_{2g}^5e_g^{1-x}$–$t_{2g}^4e_g^{2-x}$) ferromagnetically ordered state, which is followed by the high-spin state up to $x = 1.0$.

Such fascinating magnetic properties are not unique to the isotropic perovskite compound $La_{1-x}Sr_xCoO_3$; they also occur in the layered perovskite compound $La_{2-x}Sr_xCoO_4$. A zero-field nuclear magnetic resonance investigation [5] suggested that the magnetic state of $La_{2-x}Sr_xCoO_4$ suddenly transforms from an antiferromagnetic state to a ferromagnetic state when the doping concentration x is large ($x \geqslant 0.6$). The effective magnetic moment of $La_{2-x}Sr_xCoO_4$ [6] starts to decrease slowly at $x \sim 0.5$ and is followed by a sharp drop at $x \sim 0.7$, becoming an almost constant $\sim 2.6\mu_B$ afterwards. At the same time, this process is

0953-8984/00/337425+08$30.00

also accompanied by a great reduction of electrical resistivity. These experimental observations lead Moritomo *et al* to conclude that a spin-state transition of Co^{+3} takes place from the high-spin state ($t_{2g}^4 e_g^2$) to the intermediate-spin state ($t_{2g}^5 e_g^1$) at $x \sim 0.7$. However, the neutron diffraction experiment [7] gives a different physical picture and indicates that the numbers of low-spin and high-spin cobalt ions of $LaSrCoO_4$ are of the ratio of 1:1 at low temperature, which is also revealed by the optical conductivity spectra [8].

To achieve a better understanding of the magnetic properties of Sr-doped La_2CoO_4, we have previously studied the possible ground state of $LaSrCoO_4$ [9] as a function of material parameters. It was found that for a fixed Hund's coupling j, the ground state of $LaSrCoO_4$ may transform from the antiferromagnetic high-spin state ($t_{2g}^4 e_g^2$) to the ferromagnetic high-spin–low-spin ordered state ($t_{2g}^4 e_g^2$–$t_{2g}^6 e_g^0$) and finally to the nonmagnetic low-spin state ($t_{2g}^6 e_g^0$) as the crystal-field splitting Dq increases. Judging from the size of measured effective magnetic moment $\mu_{eff} \sim 2.6\mu_B$ [5, 6] and optical conductivity spectra, the most probable ground state of $LaSrCoO_4$ is found to be the high-spin–low-spin ordered state. In the present paper, we expand our investigation to the electronic structures of $La_{2-x}Sr_xCoO_4$ in the whole doping range $0.0 < x < 1.1$. The calculation is performed within the unrestricted Hartree–Fock approximation on a realistic perovskite-type lattice model. The low-spin state (LS, $t_{2g}^6 e_g^1$) and high-spin state (HS, $t_{2g}^5 e_g^2$) of La_2CoO_4 as well as all their combinations in the double cell are taken as the initial configurations, and self-consistent solutions are sought using the iteration method. To compare the relative stability of the various states, we have computed their energies as a function of the doping concentration x. It is shown that in the doping range $0.0 < x < 1.1$ two spin-state transitions occur. The first transition takes place at $x \simeq 0.39$ from the antiferromagnetic high-spin state ($t_{2g}^{5-x} e_g^2$) to the ferromagnetic high-spin state ($t_{2g}^5 e_g^{2-x}$), the second one from the ferromagnetic high-spin state to the ferromagnetic high-spin–low-spin ordered state ($t_{2g}^{5-x} e_g^2$–$t_{2g}^6 e_g^{1-x}$) at $x \simeq 0.52$, which is in qualitative agreement with experimental observation [6].

The rest of this paper is organized in the following way. In section 2 we first introduce the lattice model and the unrestricted Hartree–Fock approximation, then the real space recursion method is also briefly outlined. In section 3 we analyse the Sr doping effect on the properties of $La_{2-x}Sr_xCoO_4$ based on our numerical results. The conclusion is drawn in section 4.

2. Theoretical model and formulation

To describe the perovskite compound, the following multiband d–p model Hamiltonian [10] has been widely used. It includes the full degeneracies of the transition metal $3d$ orbitals and oxygen $2p$ orbitals as well as the on-site Coulomb and exchange interactions:

$$\mathcal{H} = \mathcal{H}_0 + \mathcal{H}_1 \tag{1a}$$

$$\mathcal{H}_0 = \sum_{im\sigma} \varepsilon_{dm}^0 d_{im\sigma}^\dagger d_{im\sigma} + \sum_{jn\sigma} \varepsilon_p p_{jn\sigma}^\dagger p_{jn\sigma} + \sum_{ijmn\sigma} (t_{ij}^{mn} d_{im\sigma}^\dagger p_{jn\sigma} + h.c.) + \sum_{ijnn'\sigma} (t_{ij}^{nn'} p_{in\sigma}^\dagger p_{jn'\sigma} + h.c.) \tag{1b}$$

$$\mathcal{H}_1 = \sum_{im} u d_{im\uparrow}^\dagger d_{im\uparrow} d_{im\downarrow}^\dagger d_{im\downarrow} + \frac{1}{2} \sum_{im \neq m'\sigma\sigma'} \tilde{u} d_{im\sigma}^\dagger d_{im\sigma} d_{im'\sigma'}^\dagger d_{im'\sigma'} - j \sum_{im\sigma\sigma'} d_{im\sigma}^\dagger \sigma d_{im\sigma'} \cdot \mathbf{S}_{im}^d. \tag{1c}$$

In equation (1) $d_{im\sigma}(d_{im\sigma}^\dagger)$ and $p_{jn\sigma}(p_{jn\sigma}^\dagger)$ denote the annihilation (creation) operators of an electron on Co-d at site i and O-p at site j, respectively, and ε_{dm}^0 and ε_p are their corresponding

on-site energies. m and n represent the orbital index and σ denotes the spin. The crystal-field splitting is included in ε^0_{dm}, i.e., $\varepsilon^0_d(t_{2g}) = \varepsilon^0_d - 4Dq$ and $\varepsilon^0_d(e_g) = \varepsilon^0_d + 6Dq$, where ε^0_d is the bare on-site energy of the d orbital. t^{mn}_{ij} and $t^{nn'}_{ij}$ are the nearest neighbour hopping integrals for p–d and p–p orbitals, they are expressed in terms of Slater–Koster parameters $(pd\sigma)$, $(pd\pi)$, $(pp\sigma)$ and $(pp\pi)$. S^d_{im} is the total spin operator of the Co ion extracting the one in orbital m, $\tilde{u} = u - 5j/2$. The parameter u is related to the multiplet averaged d–d Coulomb interaction U via $u = U + (20/9)j$.

After linearizing the Hamiltonian equation (1) using the unrestricted Hartree–Fock approximation, the following effective single particle Hamiltonian is obtained

$$\begin{aligned}\mathcal{H} = \sum_{im\sigma}[\varepsilon^0_{dm} + un^d_{im\bar{\sigma}} - \frac{j}{2}\sigma(\mu^d_t - \mu^d_m) + \tilde{u}(n^d_t - n^d_m)]d^\dagger_{im\sigma}d_{im\sigma} + \sum_{jn\sigma}\varepsilon_p p^\dagger_{jn\sigma}p_{jn\sigma} \\ + \sum_{ijmn\sigma}(t^{mn}_{ij}d^\dagger_{im\sigma}p_{jn\sigma} + h.c.) + \sum_{ijnn'\sigma}(t^{nn'}_{ij}p^\dagger_{in\sigma}p_{jn'\sigma} + h.c.).\end{aligned} \tag{2}$$

Here $n^d_{m\sigma} = \langle d^\dagger_{m\sigma}d_{m\sigma}\rangle$, $\mu^d_m = n^d_{m\uparrow} - n^d_{m\downarrow}$ and n^d_t and μ^d_t are the total electron number and magnetization of the Co-d orbitals. We have chosen the z-axis as the spin quantization axis.

For the effective single particle Hamiltonian equation (2), the density of states can be easily calculated using the real-space recursion method [11] and the Green's function is expressed as

$$G^0_{m\sigma}(\omega) = \cfrac{b_0^2}{\omega - a_0 - \cfrac{b_1^2}{\omega - a_1 - \cfrac{b_2^2}{\omega - a_2 - \cfrac{b_3^2}{\omega - a_3 - \dots}}}}. \tag{3}$$

The recursion coefficients a_i and b_i are computed from the tridiagonalization of the tight-binding Hamiltonian matrix for a given starting orbital. The multiband terminator [12] is chosen to close the continuous fractional. In order to investigate possible ground state of $La_{2-x}Sr_xCoO_4$, we have considered various ordered states in an enlarged double cell and computed 25 levels for each of the 68 independent orbitals. Our results have been checked for different levels to secure the energy accuracy better than 5 meV. The whole procedure is iterated self-consistently until convergence and the density of states is obtained by $\rho_{ms}(\omega) = -\frac{1}{\pi}ImG_{ms}(\omega)$, which allows us to compute the electron numbers and magnetic moments as well as the energies of various ordered states.

3. Numerical results and discussions

Since there have been relatively few studies on doped $La_{2-x}Sr_xCoO_4$, there are no direct experimental data on the band structure parameters, and thus these parameters have to be estimated from its counterpart $LaCoO_3$, the size of the Co–O_6 octahedron in the two compounds being essentially the same [13]. The estimated nearest neighbouring Co–O and O–O in the Co–O_6 octahedron are $(pd\sigma) = -2.0$ eV, $(pd\pi) = 0.922$ eV, $(pp\sigma) = 0.6$ eV and $(pp\pi) = -0.15$ eV, respectively. The hopping integrals between the oxygens of neighbouring layers, the $(pp\sigma)$ and $(pp\pi)$, can be obtained using the scaling relation [14] $V_{ll'm} = \eta_{ll'm}\frac{\hbar^2}{md^2}$ for different interatomic distances d. The values obtained are $(pp\sigma) = 0.334$ eV and $(pp\pi) = -0.084$ eV. The bare on-site energies of Co-d and O-p orbitals are taken as $\varepsilon^0_d = -28$ eV and $\varepsilon_p = 0$ eV. The on-site Coulomb repulsion is $U = 5.0$ eV. The crystal-field splitting and Hund's coupling are set as $Dq = 0.14$ eV and $j = 0.90$ eV, values which are

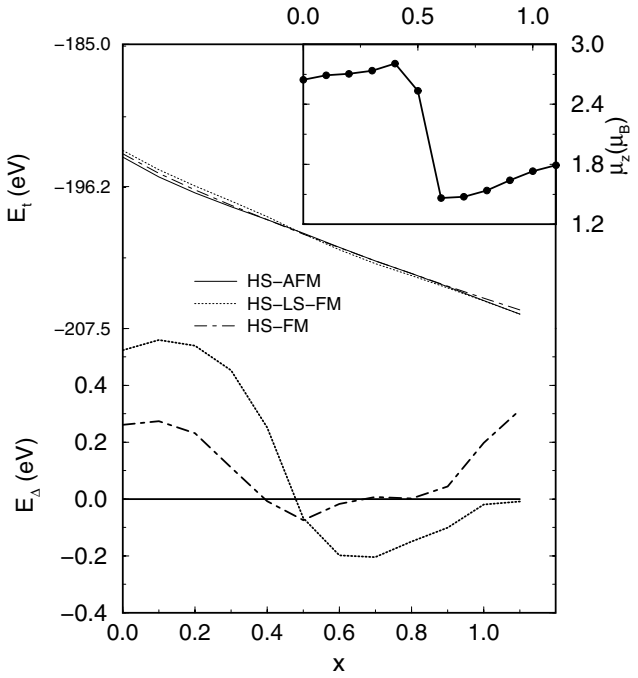

Figure 1. The total energies (E_t) and the relative energies with respect to that of the HS-AFM state (E_Δ) per double cell of the three ordered states as a function of the doping concentration x. The inset shows the doping dependence of the magnetic moment (μ) of $La_{2-x}Sr_xCoO_4$. The parameters are described in the text.

slightly larger than those in $LaCoO_3$ because the configuration of Co^{2+} in the ground state of La_2CoO_4 [15] is $t_{2g}^5 e_g^2$ (high-spin state) rather than $t_{2g}^6 e_g^1$ (low-spin state).

With the parameter set given above, the ground state of the high-spin state of La_2CoO_4 and the high-spin–low-spin ordered state of $LaSrCoO_4$ [9] are reproduced. We took the spin states of Co^{+2} of La_2CoO_4 as a reference and studied the evolution of all possible neighbouring ordered states as a function of Sr doping concentration x. It was found that only three ordered states would become the ground state in the doping range we studied; these are the antiferromagnetic high-spin ordered state (HS-AFM) for $0 < x < 0.39$, the ferromagnetic high-spin ordered state (HS-FM) for $0.39 \leqslant x < 0.52$, and the ferromagnetic high-spin–low-spin ordered state (HS–LS-FM) for $0.52 \leqslant x < 1.1$. To save space, we will concentrate our discussion on these three spin ordered states. In figure 1 we first present the total energies of the three spin ordered states as a function of doping concentration x. Since the total energies of these states are very close to each other in the doping region $0 < x < 1.1$, the relative energies with respect to that of the HS-AFM state are also plotted in the inset of figure 1. In the following, we will discuss the doping dependence of electronic structures and magnetic properties of the ground state.

As is well known, the ground state of La_2CoO_4 is an antiferromagnetic insulator [15]. Its density of states (DOS) is shown in figure 2(a) with the Fermi energy ($E_F = 0$) in the band gap. The peaks at the bottom and the top of the valence band as well as those above E_F mainly come from the t_{2g} band, while the main body of the valence band is mostly contributed by O-p orbitals. The magnetic moment is $2.65\mu_B$ and the electron occupancy of Co-d orbitals is 7.30, which is larger than that indicated by the pure ionic model due to strong covalence

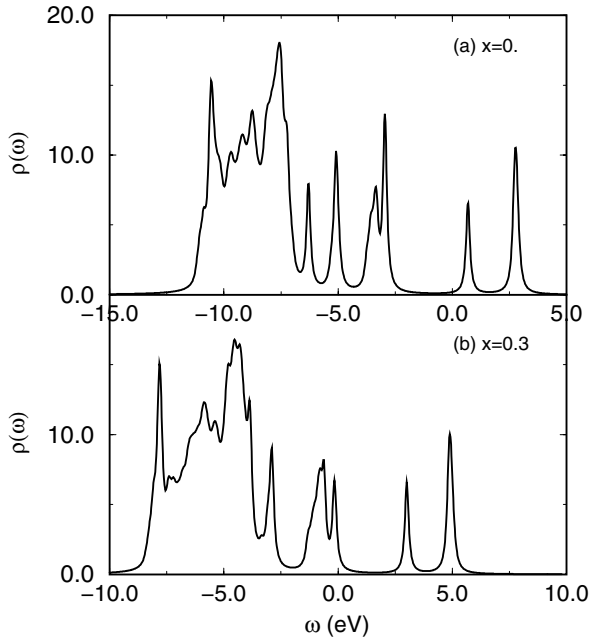

Figure 2. The total density of states of the HS-AFM ordered state for the doping concentration (a) $x = 0$, and (b) $x = 0.3$.

between Co-d and O-p orbitals. For a small to moderate doping concentration $0 < x < 0.39$, the HS-AFM state persists as the lowest energy state. However, the E_F slowly shifts from the gap region into the top of the valence band. This indicates that the system undergoes an insulator–metal transition at low temperatures, as shown in figure 2(b), since a finite density of states exists at E_F.

As the doping concentration crosses $x = 0.39$, the HS-AFM ground state is replaced by the HS-FM ordered state. This occurs because doping favours the double exchange mechanism which minimizes the system's kinetic energy. This state is also a metallic state; the typical density of states of the HS-FM ordered state is shown in figure 3 for $x = 0.5$. From the partial density of states (PDOS) of Co-d and O-p orbitals, it is seen that the main body of the valence band still comes from O-p orbitals while the peaks near E_F are contributed by Co-d orbitals. The density of states at the Fermi energy is strongly mixed with both Co-d and O-p characters. The electronic occupancy is 7.05 and magnetic moment is $2.53\mu_B$. This spin ordered state corresponds to the intermediate-spin state $(t_{2g}^5 e_g^1)$ of $LaSrCoO_4$, which was proposed to explain the sharp reduction of the magnetic moment of $La_{2-x}Sr_xCoO_4$ at $x \sim 0.7$. However, in our numerical calculation, this state only survives in a small doping region and is replaced by another spin-ordered state HS–LS-FM at $x \sim 0.52$. Indeed, the intermediate-spin configuration of Co^{+3} is energetically less favourable than that of low-spin state or high-spin state and the double exchange effect will be restrained when the doping concentration further increases, so it is impossible for the HS-FM ordered state to be stable in a large doping range.

In figure 4, we display the partial densities of states of the two different Co ions and the total density of states of the HS-LS-FM ordered state for $x = 1.0$. Obviously, the main feature of the valence band comes from the O-p band, while the total band width is mainly determined by the Co-d bands. From figure 4(a)–(c), sharp peaks mainly stem from t_{2g} orbitals and e_g

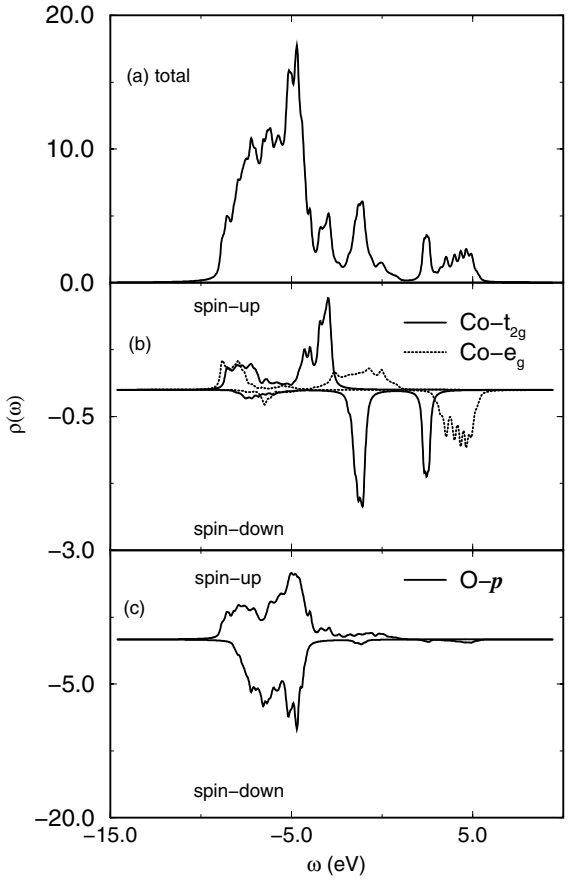

Figure 3. The density of states of the HS-FM ordered state at $x = 0.5$. (a) total DOS, (b) the PDOS for Co-d and (c) the PDOS for O-p.

bands are almost flat and broad. Moreover, the width of the HS Co-d band is broader than that of the LS Co-d band due to magnetic splitting. It is again an insulator with E_F in the band gap. The occupancy of two Co ions are 6.96 and 6.53 and their magnetic moments are $0.16\mu_B$ and $3.30\mu_B$, respectively.

Once the ground state is determined for the whole doping range, it is easy to obtain the corresponding magnetic moment that is also depicted in the inset of figure 1. Comparison with experimental measurements shows that the overall trend is correctly predicted, however the crossing points of two spin state transitions are somewhat smaller than those found in experiments. Here, temperature effect may account for this discrepancy, as our calculation is done for zero temperature while the experimental measurement is carried out at room temperature. It is noticed that the higher temperature is favourable for inducing the high-spin state since it can make the crystal-field splitting weak, thus the Hund coupling becomes more and more dominant, making the HS-AFM and HS-FM ordered states stable in a larger doping range. This physical argument is in fact proven by Demazeau *et al* [7] from their analysis on neutron diffraction and magnetic moment measurement on $LaSrCoO_4$; they found that the low-spin and high-spin cobalt ions are in a 1:1 ratio at the low temperature, while all the Co ions are in a high-spin configuration at the high temperature. Note that experiments measure the

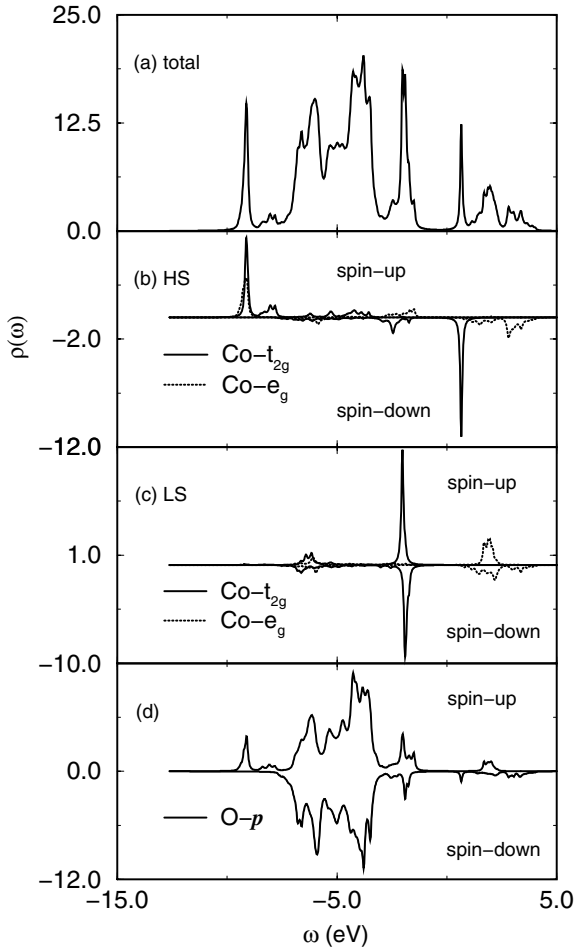

Figure 4. The density of states of the HS–LS-FM ordered state at $x = 1.0$. (a) total DOS, (b) the PDOS for high-spin Co-d, (c) PDOS for low-spin Co-d and (d) PDOS for O-p.

effective magnetic moment while our study calculates the z-components of magnetic moments, the relationship between these two quantities being approximately given by $\mu_{eff} = \sqrt{\frac{s+1}{s}}\mu_z$. We wish to point out that although the orthorhombic distortion of $La_{2-x}Sr_xCoO_4$ is neglected in our calculation, it will only slightly affect the numerical results because the orthorhombic distortion diminishes rapidly as Sr content increases and almost disappears beyond $x = 0.5$ [16].

4. Conclusion

In summary, we have studied the effect of Sr doping on the magnetic and electronic properties of layered perovskite La_2CoO_4. Within the unrestricted Hartree–Fock approximation of the multiband d-p model and real space recursion method, we calculated the various spin-ordered states from the initially different configurations of Co^{+2} of La_2CoO_4. It was found that three spin-ordered states are stable in doping range $0 < x < 1.1$ we studied; they are in the HS-

AFM ordered state for $0 < x < 0.39$, the HS-FM ordered state for $0.39 \leqslant x < 0.52$, and the HS–LS-FM ordered state for $0.52 \leqslant x < 1.1$. The doping dependence of the magnetic moment we obtained is in an overall agreement with the experimental measurement.

Acknowledgments

We acknowledge with thanks the CPU time on the SGI ORIGIN 2000 of Laboratory of Computational Condensed Matter Physics. The present work is supported in part by the National Natural Science Foundation of China under grant No NNSF 19677202. The partial financial support from the key research project in 'Climbing Program' by the National Science and Technology Commission of China is also warmly acknowledged.

References

[1] See e.g.,
Bhide V G, Rajoria D S, Jadhao V G, Rama Rao G and Rao C N R 1975 *Phys. Rev.* B **12** 2832
Golovanov V, Mihaly L and Moodenbaugh A R 1996 *Phys. Rev.* B **53** 8207
Ravindran P, Korzhavyi P A, Fjellvag H and Kjekshus A 1999 *Phys. Rev.* B **60** 16 423
[2] Chainani A, Mathew M and Sarma D D 1992 *Phys. Rev* B **46** 9976
[3] Raccah P M and Goodenough J B 1967 *J. Appl. Phys.* **39** 1209
Mahendiran R, Raychaudhuri A K, Chainani A and Sarma D D 1995 *J. Phys.: Condens. Matter* **7** L561
[4] Zhuang M, Zhang W Y, Zhou T and Ming N 1999 *Phys. Lett.* A **255** 354
[5] Furukawa Y, Wada S and Yamada Y 1993 *J. Phys. Soc. Japan* **62** 1127
[6] Moritomo Y, Migashi K, Matsuda K and Nakamura A 1997 *Phys. Rev.* B **55** 14 725
[7] Demazeau G, Courbin P, Le Flem G, Pouchard M, Hagenmuller P, Soubeyroux J L, Main I G and Robins G A 1979 *Nouv. J. Chim.* **3** 171
[8] Moritomo Y, Arima T and Tokura Y 1995 *J. Phys. Soc. Japan* **64** 4117
[9] Wang J, Zhang W Y and Xing D Y 2000 Unpublished
[10] Mizokawa T and Fujimori A 1996 *Phys. Rev.* B **54** 5368
[11] Heine V, Haydock R and Kelly M J 1980 *Solid State Physics: Advances in Research and Applications* vol 35, ed H Ehrenreich, F Seitz and D Turnbull (New York: Academic) p 215
[12] Haydock R and Nex C M M 1984 *J. Phys.* C **17** 4783
[13] Matsuura T, Tabuchi T, Mizusaki J, Yamauchi S and Fueki K 1988 *J. Phys. Chem. Solid* **49** 1409
[14] Harrison W A 1980 1989 *Electronic Structure and the Properties of Solids* (San Fransisco: W H Freeman)
[15] Yamada K, Matsuda M, Endoh Y, Keimer B, Birgeneau R J, Onodera S, Mizusaki J, Matsuura T and Shirane G *Phys. Rev.* B **39** 2336
Furukawa Y, Wada S, Kajitani T 1999 *J. Phys. Soc. Japan* **68** 346
[16] Matsuura T, Tabuchi J, Mizusaki J, Yamauchi S and Fueki K 1988 *Chem. J. Phys. Solid* **49** 1403